

Effect of short range order on electronic and magnetic properties of disordered Co based alloys

Subhradip Ghosh[†], Chhanda Basu Chaudhuri[†], Biplab Sanyal[†] and Abhijit Mookerjee[‡]

[†]S.N.Bose National Centre for Basic Sciences, JD Block, Sector 3, Salt Lake City, Calcutta 700091, India

[‡] Department of Physics, Brock University, St. Catharines, Ontario L2S 3A1, Canada.

Abstract. We here study electronic structure and magnetic properties of disordered CoPd and CoPt alloys using Augmented Space Recursion technique coupled with the tight-binding linearized muffin tin orbital (TB-LMTO) method. Effect of short range ordering present in disordered phase of alloys on electronic and magnetic properties has been discussed. We present results for magnetic moments, Curie temperatures and electronic band energies with varying degrees of short range order for different concentrations of Co and try to understand and compare the magnetic properties and ordering phenomena in these systems.

1. Introduction

The magnetic and chemical interactions in solid solutions, their interdependence and the role they play in determining the electronic and magnetic properties of transition metal alloys have been the subject of extensive experimental investigation [1]. Several phenomenological models based on statistical thermodynamic aspects of phase stability are available to describe the interplay between magnetism and spatial order [2] -[5].

Apart from this, there is one more approach of understanding the interplay between magnetism and ordering in transition metal alloys which involves investigation of the influence of local environment on electronic and magnetic properties of these alloys. A considerable amount of literature exists concerning the local(short-range)order in

transition metal alloys obtained through measurements of X-ray or neutron diffuse scattering, nuclear magnetic resonance and Mossbauer spectroscopies [6, 7, 8, 9]. In order to explain the experimental results and describe the inhomogeneous character of magnetism in these alloys many phenomenological models [10] as well as electronic structure calculations based on both zero and finite temperature models[11] have been elaborated. The effect of local environment in disordered alloys can be described in terms of short-range order(SRO) because the degree of SRO determines the extent to which spatial correlations exist in these systems. This approach has been adopted by many workers in recent times in the framework of *ab-initio* electronic structure calculations [12, 13, 14].

The macroscopic state of SRO for a disordered binary alloy is characterized by Warren-Cowley [15] SRO parameter which is given by

$$\alpha_r^{AB} = 1 - \frac{P_r^{AB}}{y} \quad (1)$$

where the A atom is at the center of the r^{th} shell, y denotes the macroscopic concentration of species B and P_r^{AB} is the pair probability of finding a B atom anywhere in the r^{th} shell around an A atom.

In the above mentioned approach, the workers either calculated the SRO parameters for a certain degree of disorder using first principles techniques and investigated the effect on ordering behavior of the systems[13, 16] or extracted the SRO parameters from experiments and observed its effect on electronic structure and properties[12, 14]. In this communication, we present the effect of SRO on the magnetic properties and the ordering behaviour of Co based alloys. For our investigations, we have chosen $\text{Co}_x\text{Pt}_{1-x}$ and $\text{Co}_x\text{Pd}_{1-x}$ alloys. Both the systems have been studied extensively over the years. In recent times they have received special attention due to their potentiality of being used as a recording medium in a new generation of storage devices. For these reasons lots of

work on optical and magneto-optical characterization of these systems are available in recent literatures [17]. Theoretical calculations include anisotropic electrical resistivity studies by Ebert *et al* [18], investigation of electronic structure and magnetic properties of ordered CoPt alloys by Kashyap *et al* [19], study of magnetism in disordered CoPt alloys by Ebert *et al* [20] and calculation of ground state properties of CoPt by Shick *et al* [21]. But, the interesting problem of interrelations of magnetism and local ordering has failed to draw much attention. The interplay between these two phenomena is quite complicated which has been studied experimentally by Sanchez *et al* [22]. To our knowledge no such investigation has been done so far for CoPd. Hence, in this work we make an attempt to understand the influence of short-range order on magnetic and electronic properties in these systems from a first principles viewpoint. Our purpose is to understand and compare these iso-electronic systems with respect to their responses to degree of short range ordering. In particular, we look at the behaviour of partial and average magnetic moments, Curie temperatures and band energies with varying alloy compositions and degrees of SRO.

2. Theoretical Details

Our calculations are based on the generalized augmented space recursion (ASR) technique [23, 24, 25]. The effective one electron Hamiltonian within the local spin density approximation (LSDA) is constructed in the framework of the tight-binding linearized muffin tin orbitals (TB-LMTO) method [26]. The Hamiltonian is sparse and therefore suitable for the application of the recursion method of Haydock *et al* [?]. The ASR allows us to calculate the configuration of the Green functions including short ranged ordering in the Hamiltonian parameters. It does so by augmenting the Hilbert space spanned by the tight-binding basis by the configuration space of the random

Hamiltonian parameters. The configuration average is expressed *exactly* as a matrix element in the augmented space. Details of this methodology has been presented in an earlier paper [27]. Here we shall quote the key results of generalized TBLMTO-ASR for short-ranged ordering. The augmented space Hamiltonian with short ranged order is written as

$$\begin{aligned}
\hat{H} = & H_1 + H_2 \sum_R P_R \otimes P_{\downarrow}^R + H_3 \sum_R P_R \otimes (T_{\downarrow\uparrow}^R + T_{\uparrow\downarrow}^R) \\
& + H_4 \sum_R \sum_{R'} T_{RR'} \otimes \mathcal{I} + \alpha H_2 \sum_{R''} P_{R''} \otimes P_{\downarrow}^1 \otimes (P_{\uparrow}^{R''} - P_{\downarrow}^{R''}) \\
& + H_5 \sum_{R''} P_{R''} \otimes P_{\downarrow}^1 \otimes (T_{\uparrow\downarrow}^{R''} + T_{\downarrow\uparrow}^{R''}) \\
& + H_6 \sum_{R''} P_{R''} \otimes P_{\downarrow}^1 \otimes (T_{\uparrow\downarrow}^{R''} + T_{\downarrow\uparrow}^{R''}) \\
& + \alpha H_2 \sum_{R''} P_{R''} \otimes (T_{\uparrow\downarrow}^1 + T_{\downarrow\uparrow}^1) \otimes (P_{\uparrow}^{R''} - P_{\downarrow}^{R''}) \\
& + H_7 \sum_{R''} P_{R''} \otimes (T_{\uparrow\downarrow}^1 + T_{\downarrow\uparrow}^1) \otimes (T_{\uparrow\downarrow}^2 + T_{\downarrow\uparrow}^2)
\end{aligned} \tag{2}$$

where R'' belong to the set of nearest neighbours of the site labelled 1i, at which the local density of states will be calculated. P 's and T 's are the projection and transfer operators either in the space spanned by the tight-binding basis $\{|R\rangle\}$ or the configuration space associated with the sites R , $\{|\uparrow_R\rangle, |\downarrow_R\rangle\}$ as described in [27]. The different terms of the Hamiltonian are given below.

$$H_1 = A(C/\Delta)\Delta_{\lambda} - (EA(1/\Delta)\Delta_{\lambda} - 1)$$

$$H_2 = B(C/\Delta)\Delta_{\lambda} - EB(1/\Delta)\Delta_{\lambda}$$

$$H_3 = F(C/\Delta)\Delta_{\lambda} - EF(1/\Delta)\Delta_{\lambda}$$

$$H_4 = (\Delta_{\lambda})^{-1/2} S_{RR'} (\Delta_{\lambda})^{-1/2}$$

$$H_5 = F(C/\Delta)\Delta_{\lambda} [\sqrt{(1-\alpha)x(x+\alpha y)} + \sqrt{(1-\alpha)y(y+\alpha x)} - 1]$$

$$\begin{aligned}
H_6 &= F(C/\Delta)\Delta_\lambda[y\sqrt{(1-\alpha)(x+\alpha y)/x} + x\sqrt{(1-\alpha)(y+\alpha x)/y} - 1] \\
H_7 &= F(C\Delta)\Delta_\lambda[\sqrt{(1-\alpha)y(x+\alpha y)} - \sqrt{(1-\alpha)x(y+\alpha x)}] \\
A(Z) &= xZ_A + yZ_B \\
B(Z) &= (y-x)(Z_A - Z_B) \\
F(Z) &= \sqrt{xy}(Z_A - Z_B)
\end{aligned} \tag{3}$$

α is the nearest neighbour Warren-Cowley parameter described earlier. λ labels the constituents. C 's and Δ 's are the potential parameters describing the atomic scattering properties of the constituents and S is the screened structure constant describing the underlying lattice which is fcc in the present case. For convenience, all the angular momentum labels have been suppressed, with the understanding that all potential parameters are 9×9 matrices. First of all, we note that in absence of short-ranged order ($\alpha = 0$), the terms H_5 to H_7 disappear and the Hamiltonian reduces to the standard one described earlier [27].

The initial TB-LMTO potential parameters are obtained from suitable guess potentials as described in the article by Andersen *et al* [28]. In subsequent iterations the potentials parameters are obtained from the solution of the Kohn-Sham equation

$$\left\{ -\frac{\hbar^2}{2m}\nabla^2 + V^{\nu\sigma} - E \right\} \phi_\sigma^\nu(r_R, E) = 0 \tag{4}$$

where,

$$V^{\lambda\sigma}(r_R) = V_{core}^{\lambda\sigma}(r_R) + V_{har}^{\lambda\sigma}(r_R) + V_{xc}^{\lambda\sigma}(r_R) + V_{mad} \tag{5}$$

here λ refers to the species of atom sitting at R and σ the spin component. The electronic position within the atomic sphere centered at R is given by $r_R = r - R$. The core potentials are obtained from atomic calculations and are available for most atoms. For the treatment of the Madelung potential, we follow the procedure suggested by

Drchal *et al* [29]. We choose the atomic sphere radii of the components in such a way that they preserve the total volume on the average and the individual atomic spheres are almost charge neutral. This ensures that total charge is conserved, but each atomic sphere carries no excess charge. In doing so, we had to be careful so that the spheres do not overlap much to violate the atomic sphere approximation.

The local charge densities are given by :

$$\rho_\sigma^\lambda(r) = (-1/\pi) \Im m \sum_L \int_{-\infty}^{E_F} dE \ll G_{LL}^{\lambda\sigma}(r, r, E) \gg \quad (6)$$

Here λ is either A or B . The local magnetic moment is

$$m^\lambda = \int_{r < R_{WS}} d^3r [\rho_\uparrow(r) - \rho_\downarrow(r)]$$

The Curie temperature T_C can be calculated using Mohn-Wolfarth (MW) model [31] from the expression

$$\frac{T_C^2}{T_C^{S^2}} + \frac{T_C}{T_{SF}} - 1 = 0$$

where, T_C^S is the Stoner Curie temperature calculated from the relation

$$\langle I(E_F) \rangle \int_{-\infty}^{\infty} N(E) \left(\frac{\delta f}{\delta E} \right) dE = 1 \quad (7)$$

$\langle I(E_F) \rangle$ is the concentration averaged Stoner parameter. The parameters of pure elements are obtained from the earlier calculations [32], $N(E)$ is the density of states per atom per spin [33] and f is the Fermi distribution function. T_{SF} is the spin fluctuation temperature given by,

$$T_{SF} = \frac{m^2}{10k_B \langle \chi_0 \rangle} \quad (8)$$

$\langle \chi_0 \rangle$ is the concentration weighted exchange enhanced spin susceptibility at equilibrium and m is the averaged magnetic moment per atom. χ_0 (pure elements) is calculated using the relation by Mohn [31] and Gersdorf [34]:

$$\chi_0^{-1} = \frac{1}{2\mu_B^2} \left(\frac{1}{2N^\uparrow(E_F)} + \frac{1}{2N^\downarrow(E_F)} - I \right)$$

I is the Stoner parameter for pure elements and $N^\uparrow(E_F)$ and $N^\downarrow(E_F)$ are the spin-up and spin-down partial density of states per atom at the Fermi level for each species in the alloy.

3. Computational Details

For all the calculations, we have used a real space cluster of 400 atoms and an augmented space shell upto the sixth nearest neighbour from the starting state. Eight pairs of recursion coefficients were determined exactly and the continued fraction was appended with the analytic terminator of Luchini and Nex [35]. In an earlier paper, Ghosh *et al* [36] have shown the convergence of the related integrated quantities, like the Fermi energy, the band energy, the magnetic moments and the charge densities, within the augmented space recursion. The convergence tests suggested by the authors were carried out to prescribed accuracies. We noted that at least eight pairs of recursion coefficients were necessary to provide Fermi energies and magnetic moments to required accuracies. We have reduced the computational burden of the recursion in the full augmented space by using the local symmetries of the augmented space to reduce the effective rank of the invariant subspace in which the recursion is confined [30] and using the seed recursion methodology [37] with fifteen energy seed points uniformly across the spectrum. The exchange-correlation potential of Von Barth and Hedin has been used. s, p and d orbitals were used to construct the basis functions and scalar relativistic corrections were included.

4. Results and Discussion

We have performed total energy calculations for CoPd and CoPt alloys for several concentrations of Co to obtain the ground state lattice parameters. Energy convergence

was set for 0.01 mRyd. The results are shown in Fig. 1. It is seen that for both CoPd and CoPt, there is a deviation from Vegard's law values (shown by dashed lines) though the trends are same. In both the cases, equilibrium lattice parameters decrease with the increase in Co concentrations. Shick *et al* [21] obtained the equilibrium lattice parameter for $\text{Co}_{50}\text{Pt}_{50}$ to be 7.049 a.u. using fully relativistic TBLMTO-CPA in frozen core approximation. Both their value and our calculated value of 6.921 a.u. are less than the experimental lattice parameter of 7.10 a.u. [39]. This is not surprising as LSDA invariably overestimates bonding.

Results for magnetic moments of $\text{Co}_x\text{Pd}_{1-x}$ are shown in Fig. 2(a) while that of $\text{Co}_x\text{Pt}_{1-x}$ are shown in Fig. 2(b). It is seen that both Pd and Pt sites also acquire some induced moments from Co. Local magnetic moments of Co go down with increasing Co concentration but the changes are not significant. This is observed in ordered alloys too [19]. This is a signature of weak local environmental effects on electronic structure. According to the calculation of Shick *et al* , the averaged and partial moments of Co and Pt in $\text{Co}_{50}\text{Pt}_{50}$ are 1.066, 1.787 and $0.345 \mu_B$ respectively. We get the values of 1.049, 1.852 and $0.24 \mu_B$ for the same while both of the values for averaged magnetic moments are close to the experimental value of $1.05 \mu_B$ [39]. Theoretical results using other techniques are not available for $\text{Co}_x\text{Pd}_{1-x}$ systems. But, our results for both the systems agree well with experimental [39]. As expected the LSDA estimate of the exchange field and hence the local magnetic moment is always larger than experimental values.

The value of Warren-Cowley SRO parameter for A_xB_y alloy is given by $-(x/y) \leq \alpha < 1$ where $\alpha = -(x/y)$ implies full short-range ordering and $\alpha = 1$ implies complete segregation. In our case we have taken our $\alpha = -0.2$ which is valid for the whole range of concentrations. The results for magnetic moments of CoPd and CoPt systems have been shown in dashed lines of Figs. 2(a) and 2(b) respectively. The results show that

the effect of SRO included through the given value of α on average magnetic moment is pretty weak. The difference in values of partial moments in the SRO state and fully disordered state is not uniform across the concentration axis for both the systems though the average moment in the SRO state is always less than that of fully disordered state. In case of CoPd, there is a crossover of partial moment value of both Co and Pd at certain concentrations with respect to the disordered value. At around 35%, the Co partial moment in the SRO state becomes less than that of disordered phase and this trend follows for the higher concentrations of Co. For Pd, however, the change is observed at around 55% but the quantitative difference with disordered phase in case of Pd is almost negligible. Exactly the same trend is observed in case of CoPt systems. Results for MW and Stoner Curie temperatures for CoPd and CoPt are shown in Figs. 3(a) and 3(b) respectively. MW Curie temperatures for both the systems are in good agreement with the experiments [39]. On the other hand Stoner Curie temperatures are highly overestimated. This is not surprising since we should realize that Stoner Curie temperature measures the temperature at which the paramagnetic state becomes unstable rather than the magnetic transition temperature. This overestimation is much reduced in the MW model [31] which combines two extreme theories- the single particle excitation and collective particle excitations. Again, the theoretical Curie temperatures are higher than experimental values due to the same reason as described in case of magnetic moments.

The results for Curie temperatures in SRO state of CoPd and CoPt are shown in Figs. 3(a) and 3(b) by dashed lines. The Stoner Curie temperatures for both the systems are almost unaffected by SRO. The influence in MW Curie temperatures is also less. Yet, there is a difference in behaviour (quantitatively) with respect to fully disordered state at around 50% for both the systems. Around 50% of Co, the difference in magnitude of

Curie temperature of SRO state and disordered state changes from positive to negative value.

Figure 4 shows the partial densities of states for equi-atomic CoPd and CoPt alloys with SRO parameter -1.0, 0.0 and 1.0. While going from the short-ranged ordering side (-1.0) to the segregation side (1.0) we find distinct changes in local DOS. The DOS for majority and minority electrons shift relative to each other and bring change in magnetic moments. For CoPd alloy, the average magnetic moment is increased from $0.96 \mu_B/\text{atom}$ to $1.24 \mu_B/\text{atom}$ while going from $\alpha=-1.0$ to 1.0. The change is from $0.88 \mu_B/\text{atom}$ to $1.09 \mu_B/\text{atom}$ in case of CoPt.

To have a complete understanding of the ordering tendency and effect of local ordering on magnetism in these systems we now carry out calculations for the full range of α at different concentrations. Figs. 5(a), 5(b) and 5(c) show the panels containing results for magnetic moments, electronic band energies and MW Curie temperatures for $\text{Co}_{20}\text{Pd}_{80}$, $\text{Co}_{50}\text{Pd}_{50}$ and $\text{Co}_{50}\text{Pd}_{50}$ respectively. It is observed that while at 20% concentration of Co, Co partial moment decreases towards the segregation side, it shows a reverse tendency at 50% and 80%. The Pd partial moment shows a rise towards the segregation side at 20% while at 50% and 80% it remains almost at a constant magnitude. To understand this behavioral difference of Co moment at different concentrations we present results of magnetic moment at 10% and 40% of Co in Figs. 6(a) and 6(b) respectively. The results for 10% mimic that of 20% but the 40% case almost follows the higher concentration trends. This can be understood in the following way: As the system goes from ordering to the segregation side, more and more Co atoms club together to build up magnetic moment of Co but at lower concentrations ($<40\%$) a Co atom finds itself in a completely non-magnetic Pd surrounding. Therefore the situation is like a magnetic impurity in a non-magnetic host which instead of building up rather

subdues its moment as it goes towards the segregation side.

The middle panels containing the results for the band energies show that at 20% the system shows a tendency towards segregation while at 50% and 80% the tendency is towards ordering. To locate the region of the transition, figure 6(b) can be investigated which presents results on band energy for 40% Co. It is seen that at this concentration the system shows tendency towards segregation which means that the ordering behavior of the system changes between 40% and 50% of Co concentration.

The bottom panels show the variation of Curie temperature with SRO parameter. At 20% and 50% concentrations Curie temperatures are higher towards ordering side while the trend is opposite at 80%. In other words, at 20% and 50% ferromagnetic phases are stable upto higher temperatures in the ordering side while at 80% they are stable upto higher temperatures in the segregation side.

Figs. 7(a), 7(b) and 7(c) present the results for the same properties but for CoPt alloys. The nature of variation of the moments are exactly same as those of CoPd and hence can be explained using the same logic. The results for the band energies show that at 20% and 50% of Co, the system shows the tendency towards ordering while at 80% it tends to segregate. Once again to locate the region of transition the bottom panels of Figs. 8(b) and 8(c) are referenced. Here, the change in ordering behavior is observed at 60% of Co which indicates that unlike CoPd, this system has a tendency to segregate between 50% and 60% of Co. From the bottom panels of Fig. 7(a-c), it is seen that at all concentrations, Curie temperature is higher at higher band energy sides. It is indicative of the possibility that the ferromagnetic phases are stable upto a lower temperature at the minimum energy state of this system.

5. Conclusions

We have studied the effects of short range order on the magnetic and electronic properties of the $\text{Co}_x\text{Pd}_{1-x}$ and $\text{Co}_x\text{Pt}_{1-x}$ alloys using fully self consistent first principles techniques. Our results for completely disordered phases agree reasonably well with the experiments. The effect of SRO on magnetic moments, electronic band energies and Curie temperatures have been investigated in detail. CoPt shows a tendency to go to ordering state from clustering(segregation) state at around 60% of Co while CoPd shows this tendency at around 40%. The response of Curie temperature to short-range ordering is linear in CoPt in the sense that at all concentrations it attains higher value at the energetically higher SRO states. For CoPd, the response is not that linear. At 20% and 80% concentrations higher values are observed at energetically higher SRO states while at 50% higher values are observed at energetically lower SRO states.

Acknowledgments

CBC would like to thank the CSIR, India for financial assistance.

References

- [1] Cadeville M C and Morán-López J L 1987 *Physics Reports* **153** 331
- [2] Sato H.,Arrott A. and Kikuchi R. 1959 *Journal of Physics and Chemistry of solids* **10** 19; Swalin R.A., *Thermodynamcis of solids*, Wiley, New York, 1962; Vonsovskii S.V., *Magnetism*, Wiley, New York, 1974
- [3] Bieber A.,Gautier F.,Treglia G. and Ducastelle F. 1981 *Solid state comm.* **39** 149; Bieber A. and Gautier F. 1981 *Solid state comm.* **38** 1219
- [4] Bieber A. and Gautier F. 1986 *Journal of Magnetism and Magnetic Materials* **54-57** 967
- [5] Hennion M. 1983 *J. Phys. F: Met. Phys.* **13** 2351
- [6] Mirebeau L.,Cadeville M.C.,Parette G. and Campbell I.A. 1982 *J. Phys. F: Met. Phys.* **12** 25
- [7] Pierron-Bohnes V.,Cadeville M.C. and Parette G. 1985 *J. Phys. F: Met. Phys.* **15** 1441
- [8] Mirebeau I.,Hennion M. and Parette G. 1985 *Phys. Rev. Lett.* **53** 687
- [9] Pierron-Bohnes V.,Cadeville M.C. and Gautier F. 1983 *J. Phys. F: Met. Phys.* **13** 1689

[10] Jaccarino V. and Walker J.L. 1965 *Phys. Rev.* **15** 258; Marshall W. 1968 *J. Phys. C: Solid State Phys.* **1** 88; Hicks T.J. 1970 *Physics Letters* **A32** 410

[11] Hasegawa H. and Kanamori J. 1971 *J. Phys. Soc. Japan* **31** 382; Buttler W.H. 1973 *Phys. Rev. B* **8** 4499; Jo T. and Miwa H. 1976 *J. Phys. Soc. Japan* **40** 706; Jo T. 1976 *J. Phys. Soc. Japan* **40** 715; Hasegawa H. 1979 *J. Phys. Soc. Japan* **46** 1504; Hamada N. 1979 *J. Phys. Soc. Japan* **46** 1759; Kakehashi Y. 1982 *J. Phys. Soc. Japan* **51** 94

[12] Borici-Kuqo M., Monnier R. and Drchal V. 1998 *Phys. Rev. B* **58** 8355

[13] Lu Z.W., Laks D.B., Wei S.H. and Zunger A. 1994 *Phys. Rev. B* **50** 6642; Wolverton C., Ozolins V. and Zunger A. 1998 *Phys. Rev. B* **57** 4332

[14] Abrikosov I. A. *et al* 1996 *Phys. Rev. Lett.* **76** 4203

[15] Cowley J.M. 1950 *J. Appl. Phys.* **21** 24

[16] Staunton J.B., Johnson D.D. and Pinski F.J. 1994 *Phys. Rev. B* **50** 1450; Johnson D.D., Staunton J.B. and Pinski F.J. 1994 *Phys. Rev. B* **50** 1473

[17] Uba S. *et al* 1998 *Phys. Rev. B* **57** 1534; Geerts W. 1994 *et al* *Phys. Rev. B* **50** 12581; Weller D., Harp G.R., Farrow R.F.C., Cebollada A. and Sticht J. 1994 *Phys. Rev. Lett.* **72** 2097

[18] Ebert H., Vernes A. and Banhart J. 1996 *Phys. Rev. B* **54** 8479

[19] Kashyap A, Garg K B, Solanki A K, Nautiyal T and Auluck S 1999 *Phys. Rev. B* **60** 2262

[20] Ebert H, Drittler B and Akai H 1992 *Journal of Magnetism and Magnetic Materials* **104-107** 733

[21] Shick A B, Drchal V, Kudrnovský and Weinberger P 1996 *Phys. Rev. B* **54** 1610

[22] Sanchez J.M. and Morán-López 1989 *J. Phys.: Condens. Matter* **1**

[23] Mookerjee A. and Prasad R. 1993 *Phys. Rev. B* **48** 17724

[24] Saha T., Dasgupta I. and Mookerjee A. 1994 *Phys. Rev. B* **50** 13267

[25] Sanyal B., Biswas P.P., Mookerjee A., Das G.P., Salunke H. and Bhattacharya A.K. 1998 *J. Phys.: Condens. Matter* **10** 5767

[26] Andersen O K, Jepsen O and Glotzel 1985 *Highlights of Condensed-Matter Theory*, edited by Bassani F, Fumi F and Tosi M P (North-Holland, New York), p. 59

[27] Biswas P.P., Sanyal B., Fakhruddin M., Halder A., Mookerjee A. and Ahmed M. 1995 *J. Phys.: Condens. Matter* **7** 8569

[28] Andersen O.K. and Jepsen O. 1984 *Phys. Rev. Lett.* **53** 2581

[29] Drchal V, Kudrnovský J and Weinberger P 1994 *Phys. Rev. B* **50** 7903

[30] Saha T, Dasgupta I and Mookerjee A 1996 *J. Phys.: Condens. Matter* **8** 1979

[31] Mohn P H and Wolfarth E P 1987 *J. Phys. F* **17** 2421

[32] Janak J.F. 1977 *Phys. Rev. B* **16** 255

[33] Gunnarson O 1976 *J. Phys. F* **6** 587

[34] Gersdorf R 1962 *J. Phys. Radium* **23** 726

[35] Luchini M U and Nex C M M 1987 *J. Phys. C: Solid State Phys.* **20** 3125

[36] Ghosh S, Das N and Mookerjee A 1997 *J. Phys.: Condens. Matter* **9** 10701

[37] Ghosh S., Das N. and Mookerjee A. 1999 *Modern Physics Letters B* **13** 723

[38] Kudrnovský J and Drchal V 1990 *Phys. Rev. B* **41** 7515

[39] *Magnetic properties of metals, 3d, 4d and 5d Elements, Alloys and Compounds*, edited by Wijn H P J, Landolt-Bornstein, New Series, Group III, Vol. 19, Pt. a (Springer-Verlag, Berlin, 1986)

Figure Captions

Figure 1 Equilibrium lattice parameters (in a.u.) vs. concentration of Co for (top) CoPd (bottom) CoPt alloys. The circles represent the calculated values whereas the dashed lines are for Vegard's law values.

Figure 2 Partial and averaged magnetic moments (in Bohr-magneton/atom) vs. concentration of Co in (a) CoPd (b) CoPt alloys. The full line is for disordered case and the dotted one for SRO state with $\alpha=-0.2$. The symbols represent : filled squares, filled circles and filled diamonds are for Co partial moments, averaged moments and Pd partial moments respectively. Diamonds represent the experimental values of average magnetic moment in fully disordered case.

Figure 3 Curie temperature (in Kelvin) vs. concentration of Co in (a) CoPd and (b) CoPt alloys. Panel(a): MW Curie temperature results. Full line represents fully disordered case. Dashed line represents SRO state characterized by $\alpha=-0.2$. Diamonds represent experimental points for fully disordered case. Panel(b): Stoner Curie temperature results. Full and dashed lines refer to the same results as in (a).

Figure 4 Spin and component projected local densities of states/atom of (a)-(c) Co₅₀Pd₅₀ and (d)-(f) Co₅₀Pt₅₀ alloys for SRO parameter equal to [(a) and (d)] -1.0 [(b) and (e)] 0.0 [(c) and (f)] 1.0. In all cases, the solid lines are for Co and the dashed lines are for Pd/Pt components. Vertical lines show the positions of Fermi levels.

Figure 5 Variation of properties of CoPd alloys with Warren-Cowley short ranged order parameter. (a) Co₂₀Pd₈₀ (b) Co₅₀Pd₅₀ and (c) Co₈₀Pd₂₀ alloys. Panels : (top) variation of partial and average magnetic moments (in Bohr magnetons/atom); symbols : filled circles, triangles and squares are for Co, average and Pd moments

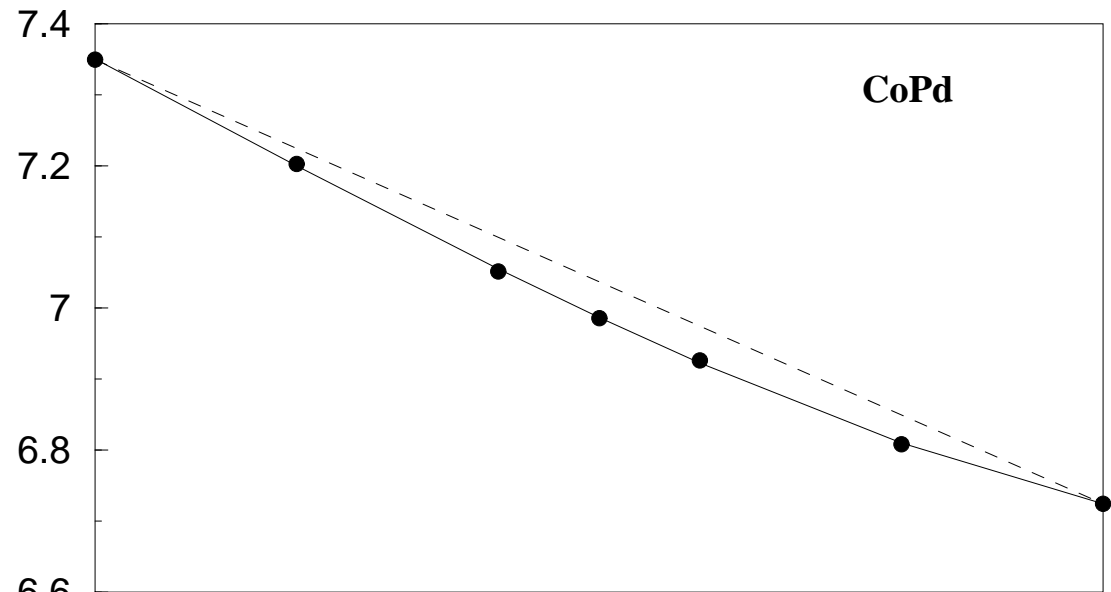
respectively. (middle) variation of band energies (in Ryd.) (bottom) variation of MW Curie temperatures (in Kelvin).

Figure 6 Variation of properties with SRO parameter for (a) $\text{Co}_{10}\text{Pd}_{90}$ and (b) $\text{Co}_{40}\text{Pd}_{60}$ alloys. Panels : (top) variation of partial and average magnetic moments ; symbols : filled circles, triangles and squares are for Co, average and Pd moments respectively. (bottom) variation of band energy.

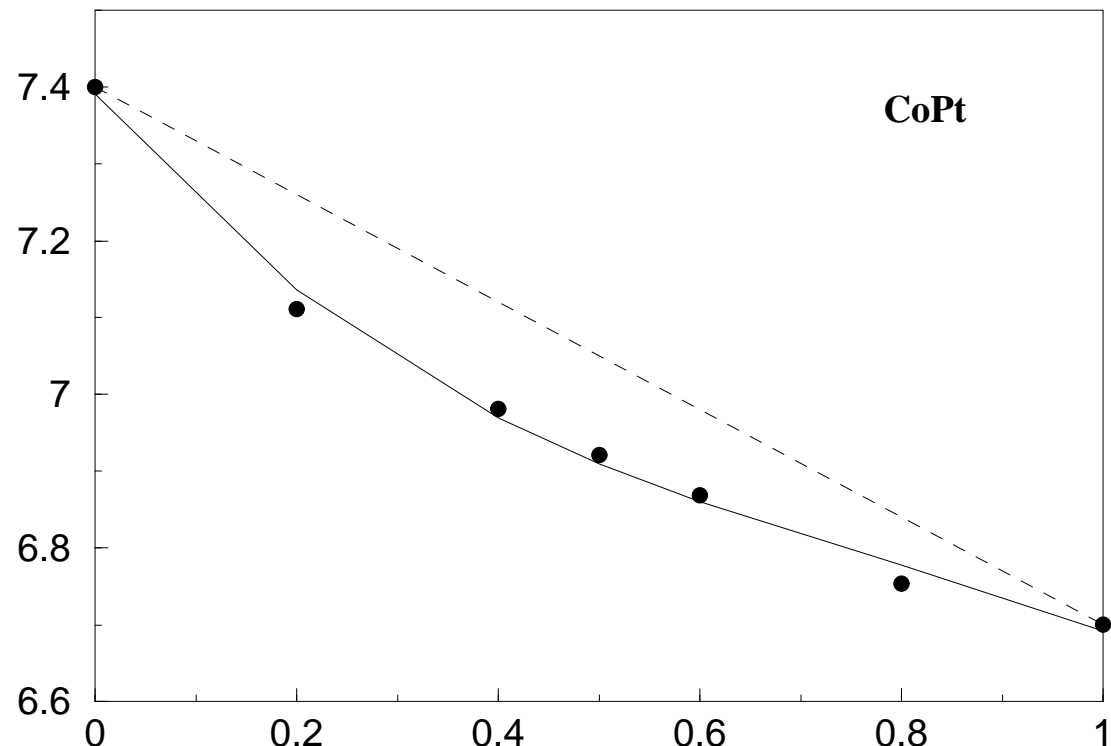
Figure 7 exactly as described for fig. 5 but for CoPt alloys.

Figure 8 Variation of properties with SRO parameter for (a) $\text{Co}_{10}\text{Pt}_{90}$ (b) $\text{Co}_{40}\text{Pt}_{60}$ and (c) $\text{Co}_{60}\text{Pt}_{40}$ alloys. Panels : (top) variation of partial and average magnetic moments ; symbols : filled circles, triangles and squares are for Co, average and Pt moments respectively. (bottom) variation of band energy.

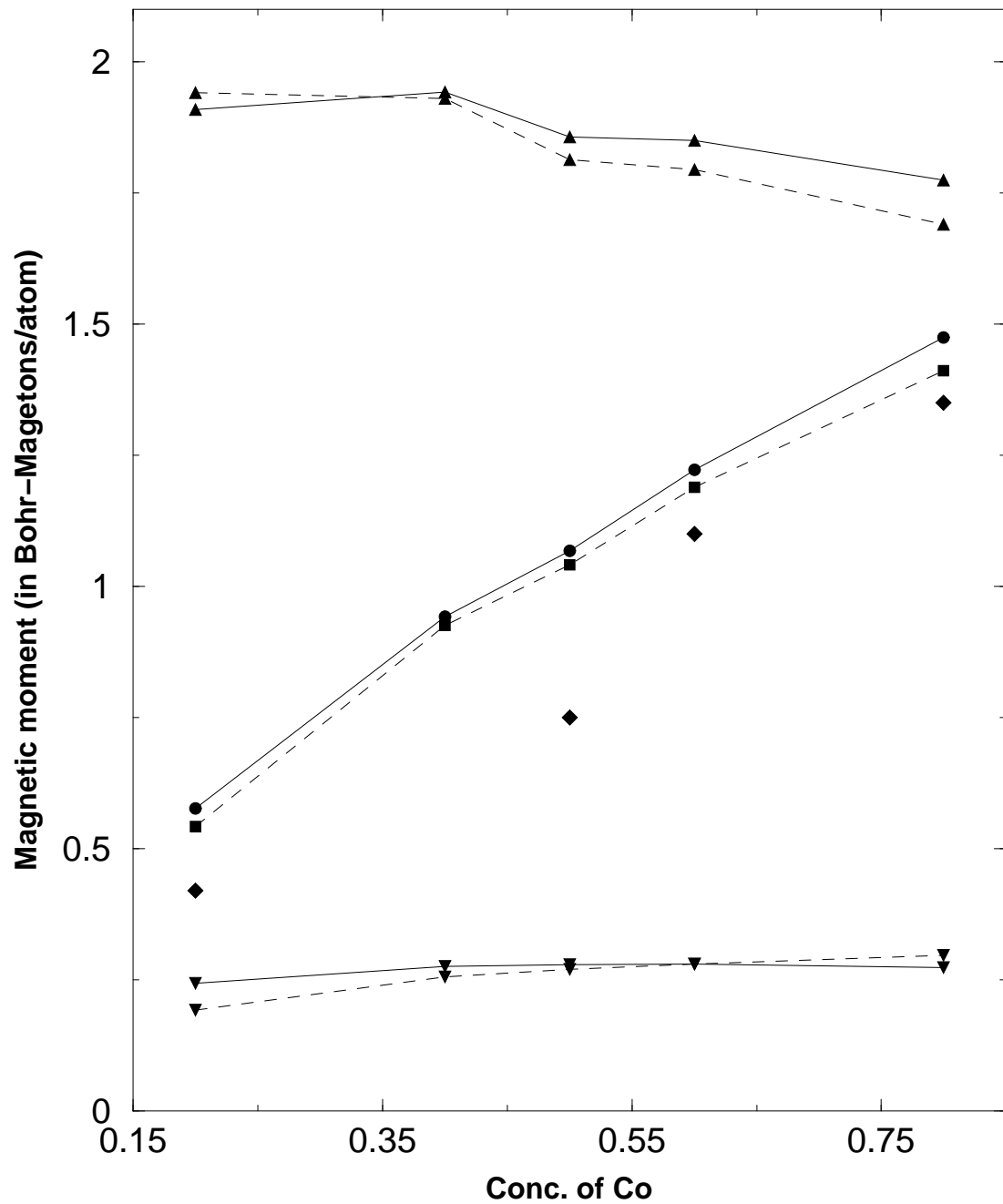
Equilibrium Lattice Parameter (a.u.)

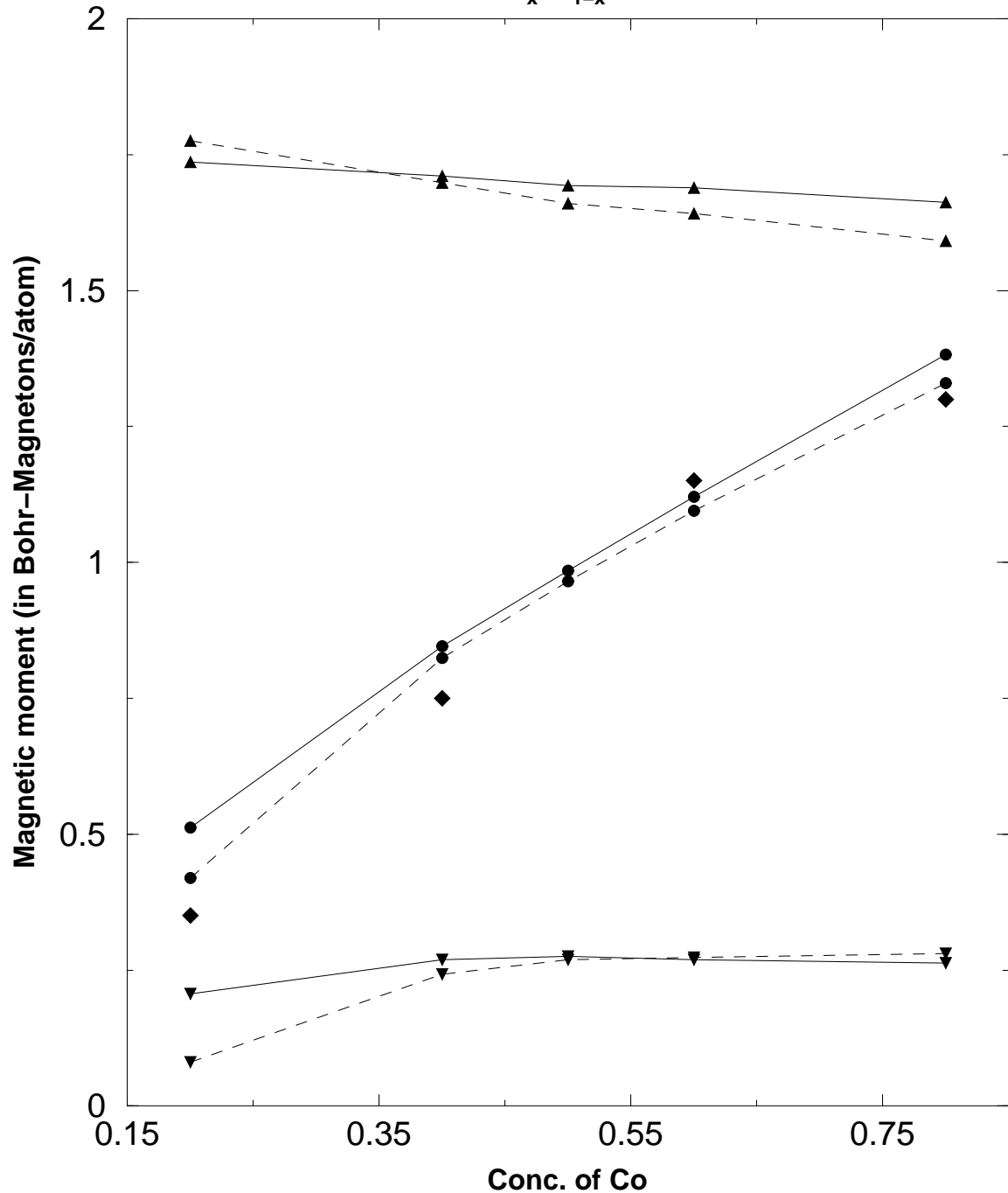


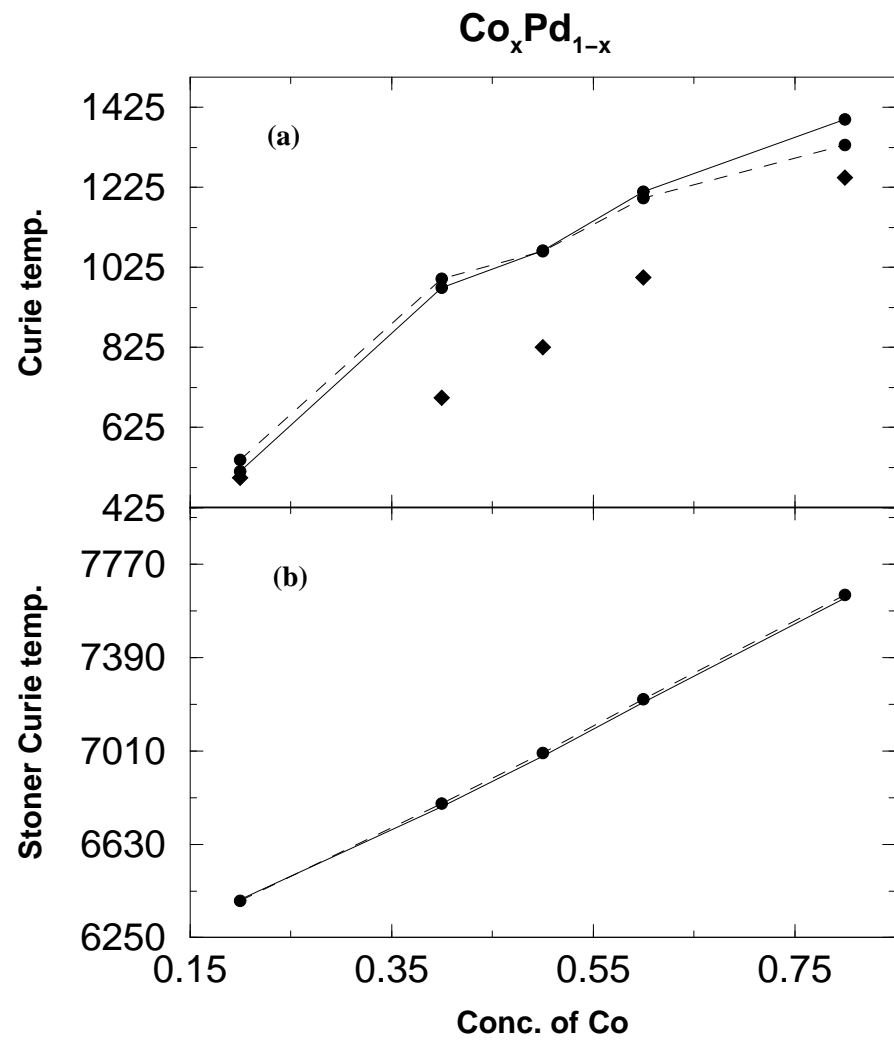
CoPt

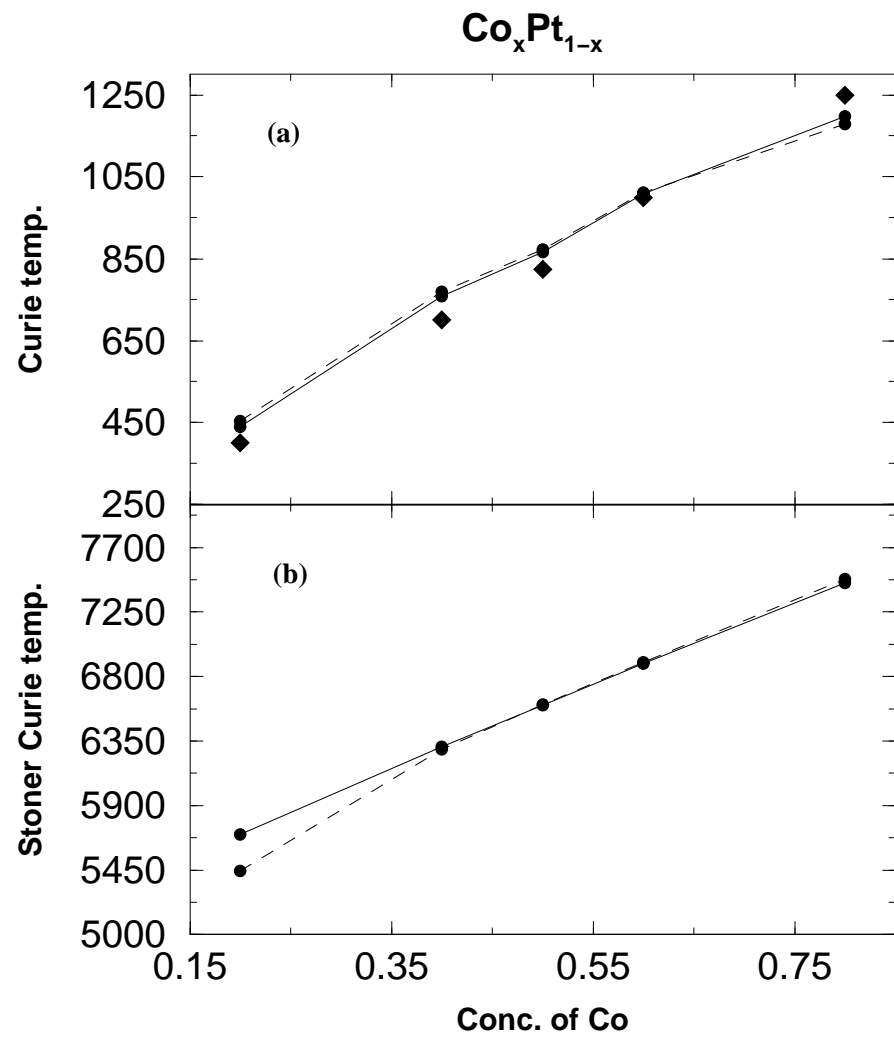


Concentration of Co

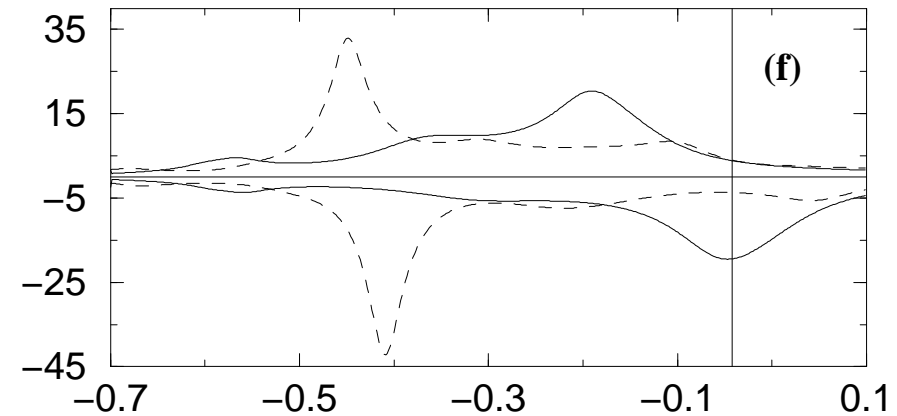
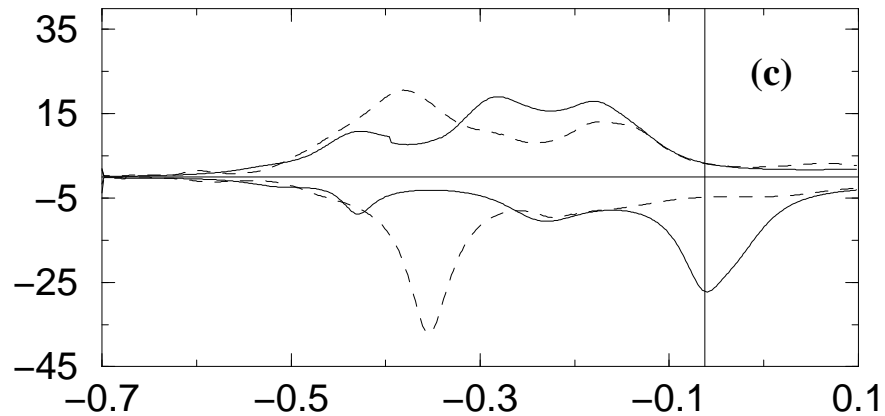
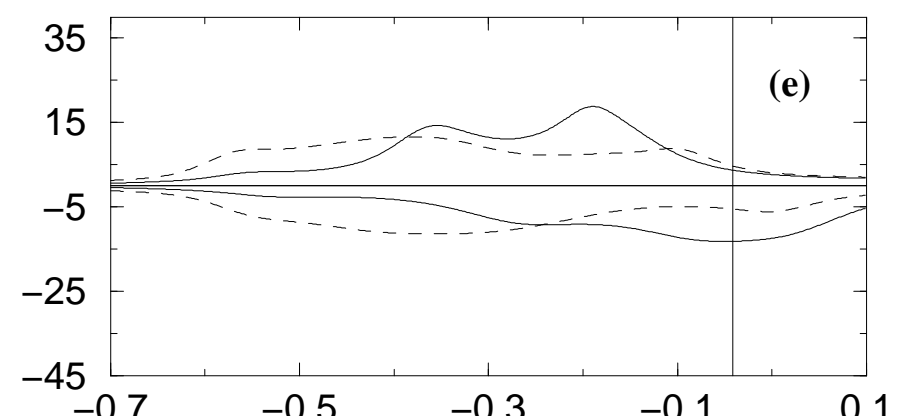
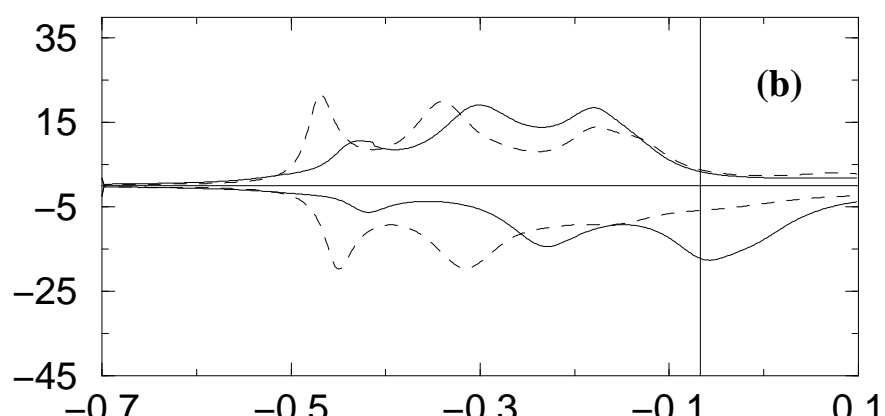
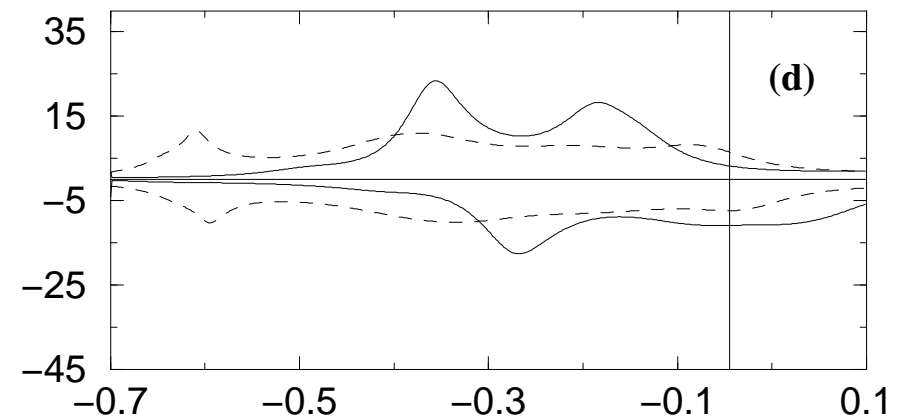
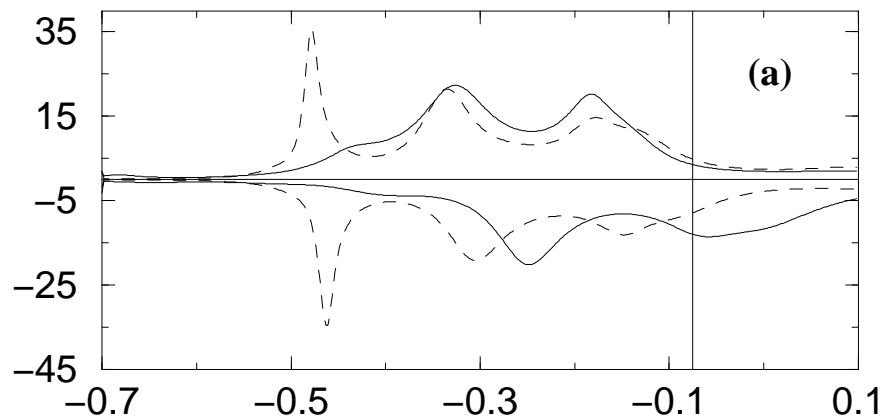


$\text{Co}_x\text{Pt}_{1-x}$ 





DOS (states/Ryd.-atom-spin)



Energy (in Ryd.)

